

A Novel Method for Indomethacin Determination Based on Graphene Loaded Nickel Oxides Nanoparticles Film

Yuxia Liu^{1,*}, Qing Huang², Cuizong Zhang³, Caiyun Liang³, Liyun Wei³, Jinyun Peng³

¹ College of Physics and Electronic Engineering, Guangxi Normal University for Nationalities, Chongzuo 532200, China

² School of Pharmacy, Henan University of Traditional Chinese Medicine, Zhengzhou 450046, China

³ College of Chemistry and Chemical Engineering, Guangxi Normal University for Nationalities, Chongzuo 532200, China

*E-mail: liuyuxiayx@163.com

Received: 15 October 2017 / Accepted: 11 December 2017 / Published: 28 December 2017

A novel method was described for sensitive voltammetric determination of indomethacin based on a graphene loaded nickel oxides nanoparticles (Gr-NiO) film by one-step electrodeposition. The as-prepared electrode (Gr-NiO/GCE) was characterized by electrochemical methods and scanning electron microscopy. The electrocatalytic properties of Gr-NiO/GCE toward the oxidation of indomethacin were analyzed via cyclic voltammetry (CV) and differential pulse voltammetry (DPV). The results indicate that the one-step prepared Gr-NiO/GCE can remarkably enhance electrocatalytic activity towards the oxidation of indomethacin. Under optimized conditions, voltammetric response of Gr-NiO/GCE was linear to indomethacin within the concentration range of 2.0×10^{-7} - 7.0×10^{-5} mol L⁻¹, with the detection limit of 5.4×10^{-8} mol L⁻¹ (S/N=3). And, the method was also applied to detect indomethacin in pharmaceutical dosage forms with wonderful satisfactory.

Keywords: Graphene; nickel oxides nanoparticles; Voltammetric sensor; indomethacin; determination

1. INTRODUCTION

Indomethacin (IMC) is a non-narcotic analgesic, non-steroidal antiinflammatory, and antipyretic drug widely used for treating or preventing the system caused by anaerobic bacteria or local infection. Even though it is completely and readily absorbed after oral administration, IMC overdose can lead to headache, vertigo, abnormal sensation, numbness of limbs, ataxia and so on [1]. Therefore, establishing sensitive and selective analytical techniques for measuring IMC in pharmaceutical and biological samples is vital necessary. It can be successfully determined by means of spectrophotography [2,3], spectrofluorimetry [4], chemiluminescence (CL) [5,6], GC[4,5], HPLC [7-10], LC-MS[11] and enzyme- linked immunosorbent assay (ELISA)[12]. Recently, electrochemical

techniques have well demonstrated for IMC detection according to the advantages of high sensitivity, less time-consumption and low cost [13-17].

Biosensors based on graphene (Gr) nanocomposite attracted wide attentions as Gr was first discovery in 2004[18-21]. Nano-sized metal oxides as nickel oxide and cobalt oxide, because of low price and excellent electrocatalytic performance, has been widely applied as supercapacitor and electrochemical sensors[22-25]. The synergetic effects between Gr and nickel particles make the Gr-supported hybrids exhibit excellent properties and improved functionalities[26-27]. Direct electrochemical deposition of nickel nanoparticles on graphene, is an attractive choice for thin film based applications as a electrochemical sensors, which rising nanocomposites with larger -area and improved electron transport[28-29]. But there is no report on the electrochemical measurement directly of IMC based on the Gr loaded nickel oxides nanoparticles (NiO) film by one-step electrodeposition.

In this work, graphene loaded nickel oxides nanoparticles modified glassy carbon electrode (Gr-NiO/GCE) by one-step electrodeposition has been developed for studying electrochemical behavior of IMC. Under optimum conditions, the differential pulse voltammetry (DPV) was fabricated for determining IMC directly, and a detection limit of 5.4×10^{-8} mol L⁻¹ (S/N=3) was achieved by this method. With such a graphene loaded nickel oxides nanoparticles film modified electrode by one-step electrodeposition, IMC in commercial tablets was evaluated with satisfactory results.

2. EXPERIMENTS

2.1. Reagents and apparatus

Reference standard of IMC was purchased from Aladdin-Reagent Company (Shanghai, China), and its standard solution (1.0×10^{-3} mol L⁻¹) was prepared by distilled water and stored at 4 °C. Graphite powder was purchased from Shanghai Shanpu Chemical Co., Ltd. (Shanghai, China). Other reagents of analytical grade were purchased from Sinopharm Chemical Reagent Co., Ltd. (China). All the chemicals were used in the direct without any further purification. Solutions were prepared using distilled water. 0.2 mol L⁻¹ Na₂HPO₄ and 0.2 mol L⁻¹ NaH₂PO₄ were to obtained the phosphate buffer solutions (PBS), the pH of which was adjusted by 0.2 mol L⁻¹ H₃PO₄ or 0.2 mol L⁻¹ NaOH.

Scanning electron microscope (SEM, ZEISS EVO18, Germany) was used to get the size and morphologies of Gr- NiO film. The electrochemical experiments were performed by a CHI660D electrochemical workstation (ChenHua Instruments Co., Shanghai, China), with a bare or NiO /GCE ($\varphi = 3$ mm) as the working electrode, a saturated calomel electrode (SCE) as the reference electrode, and a platinum wire as the counter electrode. The pH of the buffer solutions was carried out with a pHs-25 pH-meter (Leici Instrument Plant, Shanghai, China).

2.2. Preparation of the Gr-NiO/GCE

Graphite powder was used to synthesized graphite oxide (GO) via the modified Hummers method, following a previous report[30]. After the synthesis, the graphite oxide powder was obtained by filtration and drying overnight under vacuum at the temperature of 40 °C. A homogeneous GO

suspension solution was obtained by using 40 mg GO dispersed in 10 mL distilled water and treated with ultrasound. Before the electrodeposition, the GCE surface was highly polished using 0.05 μm Al_2O_3 to get a mirror finish, then sonicated in redistilled water and dried under ambient condition. Based on the reported procedure[28], Gr-NiO/GCE was prepared by dipping GCE in 4.0×10^{-2} mol L^{-1} NiSO_4 and 0.1 mol L^{-1} Na_2SO_4 solution containing 4 mg mL^{-1} GO at magnetic stirring and N_2 bubbling, followed by applying a constant potential of 1.5 V (vs. SCE) for 150 s. For comparison, NiO/GCE was prepared by the similar method dipping GCE in the solution of 4.0×10^{-2} mol L^{-1} NiSO_4 and 0.1 mol L^{-1} Na_2SO_4 , Gr /GCE was prepared by the similar method dipping GCE in 0.1 mol L^{-1} Na_2SO_4 solution containing 4 mg mL^{-1} GO.

2.3. Procedure for capsules and tablets

5 tablets were weighted accordingly and finely powdered. The amount of samples was transferred to a 100 mL capacity bottle, which containing 50 mL of PBS to get a solution with 10^{-3} mol L^{-1} . With sonicating and shaking for about 15 min, the mixture was filtered off and washed thoroughly with the same supporting electrolyte. The filtrate and washings were combined and mixed into a 100 mL volumetric flask, and then it was diluted to volume by the same solvent.

2.4. Analytical procedure

The pH 2.5 PBS was used as the supporting electrolyte during each electrochemical measurement. Under the rang from 0.6 to 1.1 V of the scanning electrode potential, DPV curves were recorded after 15 s stirring. The oxidation peak currents at 0.92 V were found for IMC. The amplitude is 0.050 V, the pulse width is 0.05 sec, and the pulse period is 0.5 sec.

3. RESULTS AND DISCUSSION

3.1. Characterization of as-prepared electrodes

Fig. 1A–C shows the SEM images of different electrodes coated with different active materials. Fig. 1A shows the surface structure of Gr-NiO coated electrode by one-step electrodeposition in the solution of 4.0×10^{-2} mol L^{-1} NiSO_4 and 0.1 mol L^{-1} Na_2SO_4 containing 4 mg mL^{-1} GO at the constant potential of 1.5 V (vs. SCE) for 150 s. The nanoparticle of NiO with the average size around 150 nm was observed on the Gr sheets. The micro-size graphene was found to cover the top of the NiO and make the connection of the covered particles. For example, the inset of Fig. 1C shows an isolated graphene flake cover on the top of NiO particles. It is interesting to note that NiO is deposited to the GCE. The TEM image of Gr sheets revealed the surface of the film was crumpled and wrinkled [31–32].

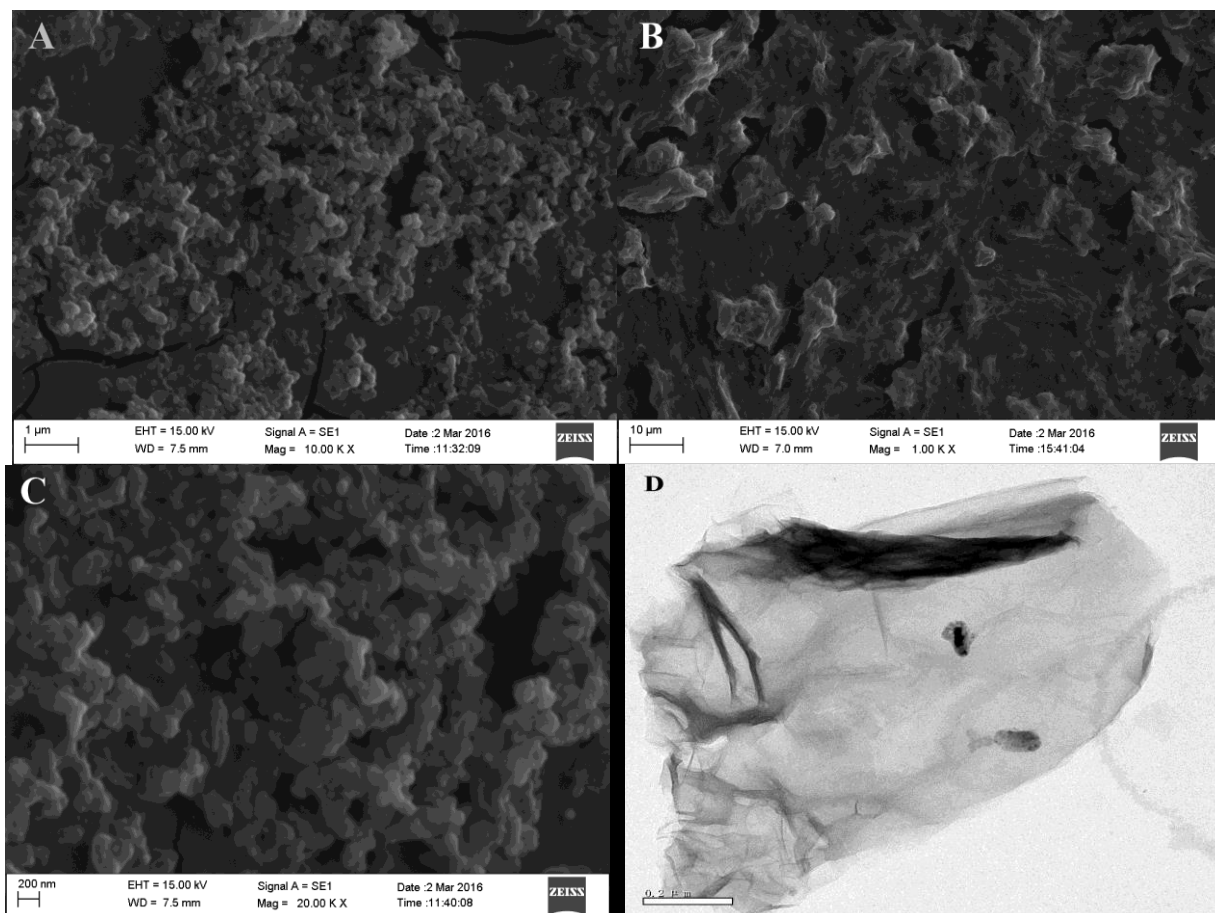


Figure 1. SEM images of Gr-NiO (a), Gr (b) and. TEM image of Gr.

3.2. Electrochemical behaviors of IMC

The voltammograms of 2.0×10^{-5} mol L⁻¹ IMC at a Gr-NiO/GCE, NiO/GCE, Gr/GCE, and bare GCE in 0.2 mol L⁻¹ (pH 7.0) PBS were presented in Fig. 2. There was no reduction peak for IMC, which suggested a totally irreversible process in the electrochemical reaction. The anodic peak potential of IMC at Gr-NiO/GCE is about 0.77V (curve 4), while it was respectively 0.76V and 0.79V at Gr/GCE (curve 4) and bare GCE (curve 2). The anodic current (I_p) of IMC was 7.75×10^{-6} A, which is about 10.4, 6.4 and 2.3 times larger than the anodic current at GCE, NiO/GCE and Gr/GCE respectively. These results clearly indicate the combination of Gr & NiO definitely increased the oxidation of IMC. It might be related to the high surface area and highly electrical conductivity of Gr. The role of NiO was also attributed to promoting the electrochemical characteristics of IMC oxidation. So Gr-NiO could be used for the oxidation of IMC.

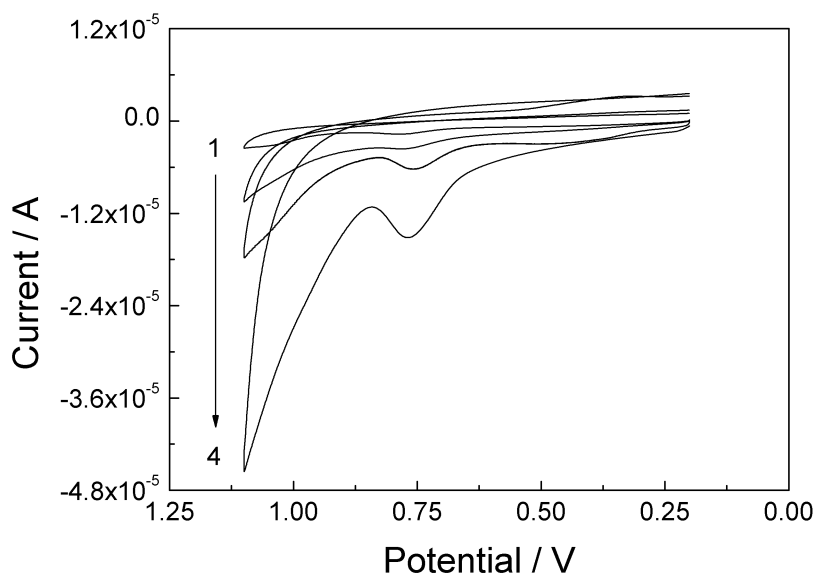


Figure 2. CVs of IMC recorded at different electrode in PBS (line 1-4: GCE, NiO/GCE, Gr/GCE, Gr-NiO/GCE), scan rate: 100 mV s⁻¹.

3.3. Effect of pH value

The effect of electrolytical pH on the cyclic voltammetric response of Gr-NiO/GCE toward the determination of IMC was studied with PBS buffered solution in different pH from 1.5 to 7.0. As can be seen in Fig. 3, the peak current remains almost constantly while pH increased from 1.5 to 2.5.

Obviously, with increasing pH from 2.5 to 7.0, the anodic current decreased greatly. Therefore a PBS solution of pH 2.5 was elected to use in the subsequent analysis.

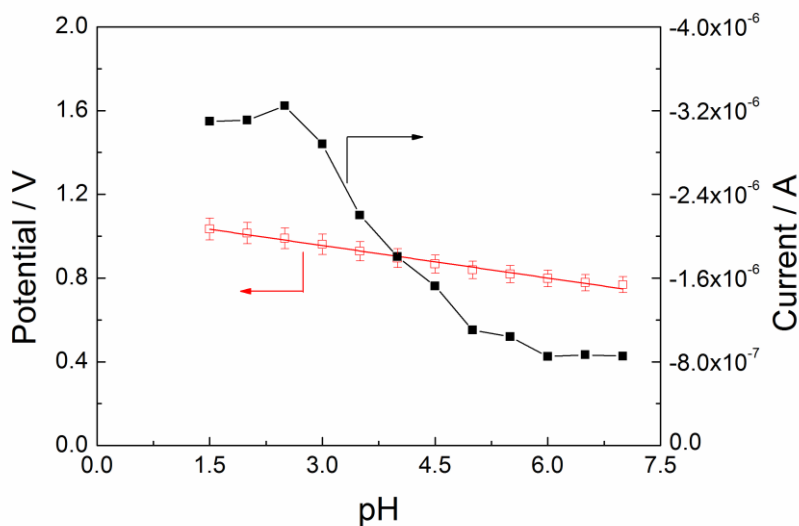


Figure 3. Effect of pH on peak current and potential of 1.0×10^{-5} mol L⁻¹ IMC

The anodic peak potential of IMC, as shown in Fig. 3, was dependent of acidity solution. The value of anodic peak potential with IMC was shifted to less positive voltage with the increase of pH, and they revealed a relationship as: E_p (V) = 1.04–0.0512 pH ($r = 0.998$). The slope of -51.2 mV pH^{-1} demonstrated that the numbers of electron transferred were equal to proton transferred in the electrochemical reaction of IMC.

3.4. Effect of scan rate

Useful information about the mechanism can be obtained on the relationship between anodic current (I_p) and scan rate. The effect of scan rate on the electrochemical behavior of IMC was studied at working electrode by cyclic voltammetry. In the range of $0.01\text{--}0.8 \text{ V s}^{-1}$, a linear relationship between anodic peak current and scan rate was acquired ($I_p = -8.52 \times 10^{-6} v - 7.71 \times 10^{-7}$, $n=18$, $r=0.9966$). The results indicated that the oxidation of IMC was controlled by adsorption.

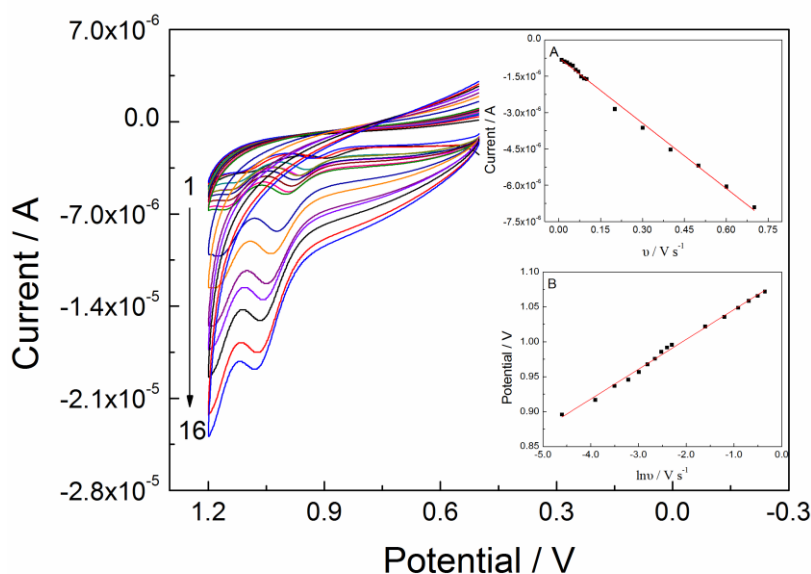


Figure 4. Effect of scan rates by CV with IMC ($1.0 \times 10^{-5} \text{ mol L}^{-1}$) in PBS (pH 2.5) (from 1 to 16: 0.01, 0.02, 0.03, 0.04, 0.05, 0.06, 0.07, 0.08, 0.09, 0.1, 0.2, 0.3, 0.4, 0.6, 0.7, 0.8, V s^{-1}); insert (A) is the I_p vs. v plot; insert (B) is the E_p vs. $\ln v$ plot.

The peak potential positively correlated with the scan rate. The peak potential’s relationship with logarithm of scan rate was found as E_p (V) = $0.0426 \ln v$ (V s^{-1}) + 1.088 ($n=18$, $r=9973$). For an irreversible oxidation electrode process [33], E_p can be defined as Equation 1.

$$E_p = E^{0'} + \frac{RT}{(1-\alpha)nF} \ln v \quad (1)$$

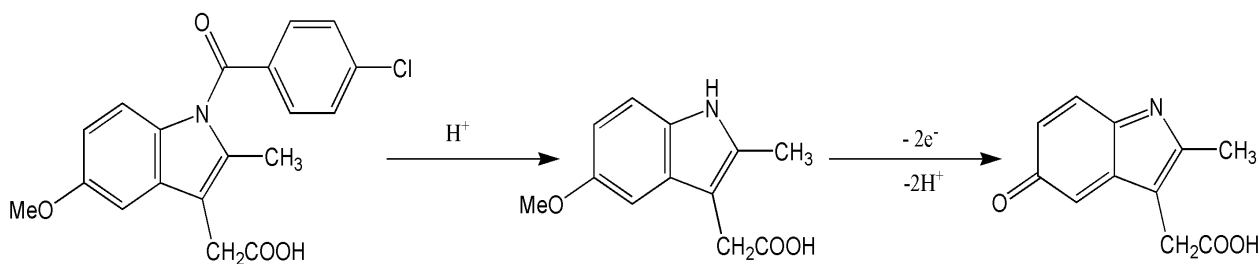
The full name or meaning of each function included in the equation is as follows:

The peak potential (E_p , V vs. SCE), the formal potential ($E^{0'}$, V vs. SCE), the universal gas constant (R , $8.314 \text{ J K}^{-1} \text{ mol}^{-1}$), the temperature (T , K), the alpha (α) signifies the coefficient in

charge-transfer for the oxidation step, n signifies the electron transfer number of electro-active material when the electrode reaction occurs, the Faraday constant (F , $96,485 \text{ C mol}^{-1}$). According to Bard and Faulkner [34], α can be given as

$$\alpha = \frac{47.7}{E_p - E_{p/2}} \text{ mV} \quad (2)$$

Half peak potential ($E_{p/2}$) represents the potential when the current reaches half the peak value. From this, the value of α and n was calculated to be 0.72 and 2.15 (approximately equal to 2) respectively. The proposed mechanism on the Gr-NiO/GCE may be depicted in Scheme 1.



Scheme 1. Proposed mechanism of IMC for electrochemical behavior on Gr-NiO/GCE

This conclusion is also bolstered by other investigations with the electrochemical reactions of IMC [13, 16].

3.5. Electrochemical impedance spectroscopy (EIS) of different electrodes

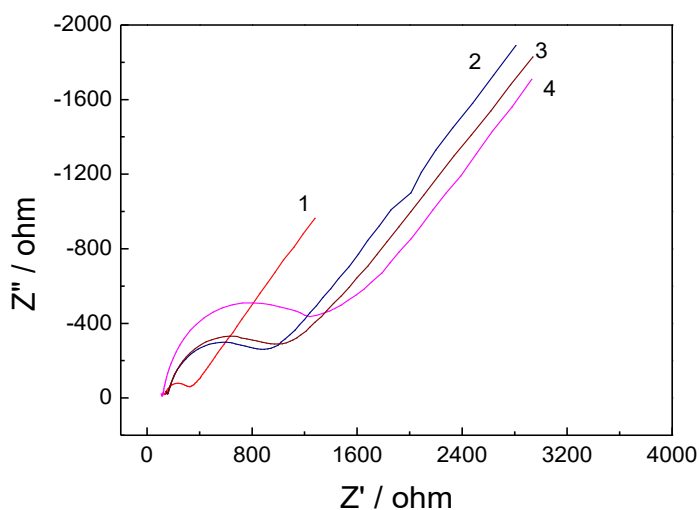


Figure 5. EIS of different electrode (line 1-4: Gr-NiO/GCE, Gr/GCE, NiO/GCE and GCE) in a solution containing $\text{K}_3[\text{Fe}(\text{CN})_6]$ ($1.0 \times 10^{-3} \text{ mol L}^{-1}$), $\text{K}_4[\text{Fe}(\text{CN})_6]$ ($1.0 \times 10^{-3} \text{ mol L}^{-1}$), and KCl (0.1 mol L^{-1}). With the applied perturbation amplitude as 0.005 V ; init E as 0.236 V , the frequencies swept as 10^5 – 1 Hz ; quiet time as 2 s .

In order to further understand the situation of electron transfer on the working electrode surface, EIS was investigated. The semicircle diameter of excellent conducting substrates can be presented by the value of the electron transfer resistance (R_{ct}).

EIS based on $1.0 \times 10^{-3} \text{ mol L}^{-1} \text{ Fe(CN)}_6^{3-/4-}$ as a redox probe for electrodes were shown in Fig. 4. At the GCE, R_{ct} can be estimated to be 1050Ω (curve 4), indicating that electron-transfer resistance is very large. The R_{ct} of Gr-NiO/GCE nearly equal to zero, which suggested the electrochemical probe was accelerated to the substrate electrodes. The result indicated that Gr and NiO film can act effectively as electron conductive bridge between the electrode and electrolyte.

3.6. Calibration curve

Compared with cyclic voltammetry, differential-pulse voltammetric mode has sharper and better peaks at lower concentrations, and it was used to determining IMC with PBS at pH 2.5 (Fig. 6). The peak potential at about 0.92 V was selected for the analysis. Under optimal operating conditions, the result shown that current (I_p) increased linearly with the increase of IMC. The calibration curves for determination were built in the range of 2.0×10^{-7} - $7.0 \times 10^{-5} \text{ mol L}^{-1}$. The linear regression equation was $I_p \text{ (A)} = -5.5 \times 10^{-8} - 4.1 \times 10^{-2} C$ ($r = 0.9986$). The limit of detection (LOD) was estimated to be $5.4 \times 10^{-8} \text{ mol L}^{-1}$ ($S/N=3$). These results provided that Gr-NiO/GCE was an appropriate methodology for the analysis of IMC. The comparison of Gr-NiO modified electrode for determining IMC with other electrodes was listed in Table 1. As can be seen, the linear range of Gr-NiO modified electrode for determining IMC is wider than other electrode except for $\text{MnO}_2\text{-Gr/GCE}$. And LOD of this work is lower than most of the previous reports in table 1. It revealed that Gr-NiO/GCE is a suitable platform for the application to detecting IMC.

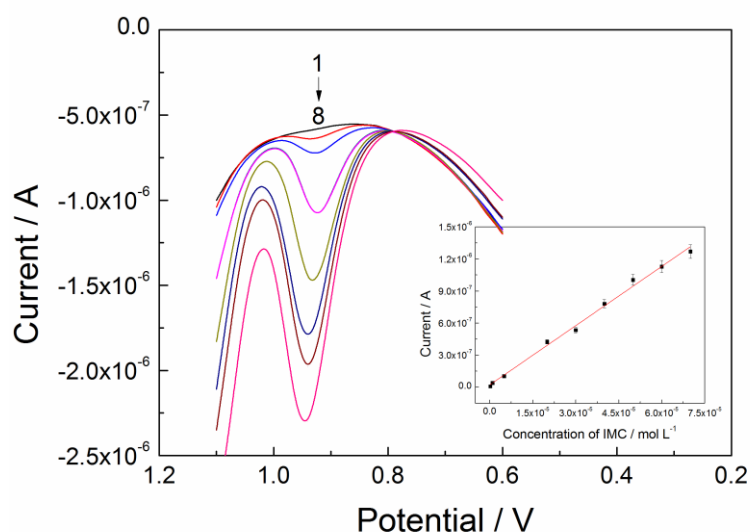


Figure 6. IMC recorded by DPV at Gr-NiO/GCE with different concentrations (from 1 to 8: 2.0×10^{-7} , 1.0×10^{-6} , 5.0×10^{-6} , 2.0×10^{-5} , 3.0×10^{-5} , 4.0×10^{-5} , 5.0×10^{-5} , 6.0×10^{-5} , $7.0 \times 10^{-5} \text{ mol L}^{-1}$). Inset is calibration curve.

Table 1. The detection of IMC between the fabricated electrode and other electrodes

Electrode	Technique	Linear range (mol L ⁻¹)	Correlation coefficient	LOD (mol L ⁻¹)	Ref.
Ni(OH) ₂ -Ni	i-t	5.0×10 ⁻⁶ -7.9×10 ⁻⁵	0.9980	1.4×10 ⁻⁶	[35]
Ni-GCE ^a	i-t	3.8×10 ⁻⁴ -1.4×10 ⁻³	0.9961	7.5×10 ⁻⁵	[36]
RB ISE ^b	-	1.0×10 ⁻⁴ -5.0×10 ⁻²	-	3.0×10 ⁻⁵	[37]
INDO-TOA ISE ^c	-	1.0×10 ⁻⁵ -1.0×10 ⁻²	-	3.2×10 ⁻⁶	[17]
Fe(III)-SBMCP ^d	DPV	2.0×10 ⁻⁷ -1.5×10 ⁻⁴	0.9995	8.0×10 ⁻⁸	[38]
EP ACBK/GCE ^e	DPV	3.0×10 ⁻⁷ -4.0×10 ⁻⁵	0.9978	9.8×10 ⁻⁸	[39]
GCE	DPSV	6.0×10 ⁻⁶ -1.0×10 ⁻⁴	-	3.8×10 ⁻⁷	[40]
GNRs-GO-CNTP/GCE	SWV	2.0×10 ⁻⁷ -9.0×10 ⁻⁷ , 2.5×10 ⁻⁶ -9.15×10 ⁻⁵	-	1.7×10 ⁻⁸	[16]
MWCNT-IL/CCE	DPV	1.0×10 ⁻⁶ -5.0×10 ⁻⁵	-	2.6×10 ⁻⁷	[15]
MWCNTs-NHNPs-MCM- 41/GCE	DPV	8.0×10 ⁻⁷ -4.0×10 ⁻⁵ , 6.0×10 ⁻⁵ -1.6×10 ⁻⁴	0.9965 0.9980	3.1×10 ⁻⁷	[14]
MnO ₂ -Gr/GCE	DPV	1.0×10 ⁻⁷ -2.5×10 ⁻⁵	0.9989	3.2×10 ⁻⁸	[13]
Gr-NiO	DPV	2.0×10 ⁻⁷ -7.0×10 ⁻⁵	0.9986	5.4×10 ⁻⁸	This work

^a Ni–curcumin modified GCE, ^b IMC-selective sensor based on Rhodamine B, ^c IMC-selective sensor based on tetraoctylammonium 1-(p-chlorobenzoyl)5-methoxy-2-methyl-3-indolylacetate, ^d Fe(III) Schiff base modified electrodes, ^e Electropolymerization of Acide Chrome Blue K on GCE,

3.7. Reproducibility, stability and interferences

Five independently working electrodes were used to measure 1.0×10⁻⁵ mol L⁻¹ IMC for investigating the fabrication reproducibility. The RSD of the peak current was 1.6%. The experimental results established that the results are reproducible.

The peak current could retain 97.5% of its original response after working electrode was stored at 4°C in humidity environment for five days, indicating that the Gr-NiO/GCE possess acceptable storage stability. In order to achieve the application of the analytical method requirements, the effect of a number of common ingredients used in drug combinations were investigated by analyzing sample solutions containing a fixed concentration of IMC (1.0×10⁻⁵ mol L⁻¹), at the same experimental conditions, spiked with various excess amount of each ingredients. In this experiment, no interference (relative error <±5%) for maltose, glucose, acetic acid, proteins, sodium chloride, barium chloride, magnesium chloride, nickel chloride and calcium chloride (>200-fold in excess over analyte concentration), uric acid, citric acid, soluble starch, dextrin, aluminium nitrate, copper sulphate, potassium chloride, zinc chloride, ammonium carbonate, sodium nitrate, sodium twelve sulfonate, cobalt sulfate (>100-fold in excess), cadmium chloride, ferric chloride, manganese sulfate (50-fold in excess), ascorbic acid (15-fold in excess) were found. These results revealed that Gr-NiO/GCE is not significantly influenced by interferences, the method might be used for IMC analysis in the pharmaceutical dosage forms.

3.8. Analytical application

As a proof of principle, the applicability of the proposed method was estimated by detecting two commercial drug samples containing IMC. Results of the IMC repair test for these drugs are shown in Table 1. The recoveries results showed that the developed methods could be applied for the quantitative analysis of trace amounts of IMC in pharmaceuticals efficiently.

Table 1. Proposed procedures were used for detecting pharmaceutical formulations

Pharmaceutical formulation ^a	Labeled values (mg/tablet)	Proposed procedures ^c (mg/tablet)	Added (mg/tablet)	Found (mg/tablet)	Recovery (%)
Tablets	25	24.2±0.5	15.0	39.3	100.7
Capsules	75	74.7±3.1	20.0	94.5	99.1

^aTablets: Batch No. A150901, Expiry date: 03/2018, from Shanxi Yunpeng Pharm.; Capsules: Batch No. 1140402, Expiry date: 03/2017, from Beijing Honglin Pharm. ^c Average of five replicate measurements ± SD.

4. CONCLUSIONS

IMC can produce a more sensitive anodic peak at Gr-NiO/GCE due to it can be adsorbed and promoted electron-transfer on the electrode. Compared with bare GCE, Gr-NiO electrode provides higher electro-active surface and lower charger transfer resistance. Under optimal operating conditions, peak currents and concentrations of IMC were linearly in a certain range. Gr-NiO/GCE exhibits high repeatability and good stability. It was revealed the proposed method could be used for the determination of IMC in medicines.

ACKNOWLEDGEMENTS

We sincerely thank the National Natural Science Foundation of China (Nos. 21465004) for the financial support. We also acknowledge support of the Guangxi Science Foundation of China (No. 2016GXNSFAA380113) for the financial support.

References

1. T.M.T. Sheehan, D.A.R. Boldy, J.A. Vale, *J. Toxicol. Clin. Toxic.*, 24 (19862) 151.
2. R.K. Maheshwari, A. Rathore, A. Agrawal, M.A. Gupta, *Pharmaceut. Methods*, 2 (2011) 184.
3. P. Nagaraja, R.A. Vasantha, H.S. Yathirajan, *J. Pharmaceut. Biomed.*, 31 (2003) 563.
4. P.C.A.G. Pinto, M.L.M.F.S. Saraiva, J.L.M. Santos, J.L.F.C. Lima, *Anal. Chim. Acta*, 539 (2005) 173.
5. F. Nie, J. Lu, Y. He, J. Du, *Talanta*, 66 (2005) 728.
6. K. Mervartova, M. Polasek, J.M. Calatayud, *Anal. Chim. Acta*, 600 (2007) 114.
7. L. Nováková, L. Matysová, L. Havlíková, P. Solich, *J. Pharmaceut. Biomed.*, 37 (2005) 899.
8. M.A. Al Zaabi, G.H. Dehghanzadeh, R.L.G. Norris, B.G. Charles, *J. Chromatogr. B*, 830 (2006) 364.
9. Y. Zhang, Z. Zhang, G. Qi, Y. Sun, Y. Wei, H. Ma, *Anal. Chim. Acta*, 582 (2007) 229.

10. K. Michail, M.S. Moneeb, *J. Pharmaceut. Biomed.*, 55 (2011) 317.
11. X. Wang, D.I. Vernikovskaya, T.N. Nanovskaya, E. Rytting, G.D.V. Hankins, M.S. Ahmed, *J. Pharmaceut. Biomed.*, 78-79 (2013) 123.
12. S. Huo, H. Yang, A. Deng, *Talanta*, 73 (2007) 380.
13. Y. Liu, Z. Zhang, C. Zhang, W. Huang, C. Liang, J. Peng, *Bull. Korean Chem. Soc.*, 37 (2016) 1173.
14. A. Babaei, A. Yousefi, M. Afrasiabi, M. Shabanian, *J. Electroanal. Chem.*, 740 (2015) 28.
15. K. Sarhangzadeh, A. A. Khatami, M. Jabbari, S. Bahari, *J. Appl. Electrochem.*, 43 (2013) 1217.
16. M. Arvand, T. M. Gholizadeh, *Sensor. Actuat. B-Chem.*, 186 (2013) 622.
17. J. Lenika, C. Wardak, *Procedia Engineering* 47 (2012) 144.
18. K.S. Novoselov, A.K. Geim, S.V. Morozov, D. Jiang, Y. Zhang, S.V. Dubonos, I.V. Grigorieva, A.A. Firsov, *Science*, 306 (2004) 666.
19. L. Wang, Y. Zhang, A. Wu, G. Wei, *Anal. Chim. Acta*, 985 (2017) 24.
20. C.I.L. Justino, A. R. Gomes, A. C.Freitas, A. C. Duarte, T. A. P. Rocha-Santos, *TrAC-Trend. Anal. Chem.*, 91 (2017) 53.
21. C. Zhu, D. Du, Y. Lin, *Biosens. Bioelectron.*, 89 (2017) 43.
22. Y. Zhang, D. Zhao, W. Zhua, W. Zhang, Z. Yue, J. Wang, R. Wang, D. Zhang, J. Wang, G. Zhang, *Sensor. Actuat. B-Chem.*, 255 (2018) 416.
23. B. B. Prasad, R. Singh, K. Singh, *Sensor. Actuat. B-Chem.*, 246 (2017) 38.
24. X. Li, X. Lu, X. Kan, *J. Electroanal. Chem.*, 799 (2017) 451.
25. G. Kaur, M. Tomar, V. Gupta., *Biosens. Bioelectron.*, 80 (2016) 294.
26. S.Darvishia, M.Souissib, F.Karimzadeha, M.Kharazihaa, R.Saharab, S.Ahadianc, *Electrochim. Acta*, 240 (2017) 388.
27. S. Ragu, S. Chen, P. Ranganathan, S. Rwei, *Int. J. Electrochem. Sci.*, 11 (2016) 9133.
28. H. Belkhalifa, F. Teodorescu, G. Quéniat, Y. Coffinier, N. Dokhan, S. Sam, A. Abderrahmani, R. Boukherroub, S. Szunerits, *Sensor. Actuat. B-Chem.*, 237 (2016) 693.
29. G. Liu, H. Chen, G. Lin, P. Ye, X. Wang, Y. Jiao, X. Guo, Y. Wen, H. Yang, *Biosens. Bioelectron.*, 56 (2014) 26.
30. W.S. Hummers, R.E. Offeman, *J. Am. Chem. Soc.*, 80 (1958) 1339.
31. H.C. Schniepp, J.L. Li, M.J. McAllister, H. Sai, M. Herrera-Alonso, D.H. Adamson, R.K. Prud'homme, R. Car, D.A. Saville, I.A. Aksay, *J. Phys. Chem. B*, 110 (2006) 8535.
32. X. Fan, W. Peng, Y. Li, X. Li, S. Wang, G. Zhang, F. Zhang, *Adv. Mater.*, 20 (2008) 4490.
33. E. Laviron, *J. Electroanal. Chem.*, 100 (1979) 263.
34. A.J. Bard, L.R. Faulkner, *Electrochemical Methods Fundamentals and Application*, 2nd ed., Wiley, 2004, p. 236.
35. M. Hajjizadeh, A. Jabbari, H. Heli, A.A. Moosavi-Movahedi, S. Haghgoo, *Electrochim. Acta* 53 (2007) 1766.
36. H. Heli, A. Jabbari, S. Majdi, M. Mahjoub, A. A. Moosavi-Movahedi, Sh. Sheibani, *J. Solid State Electrochem.* 13 (2009) 1951.
37. Z. Kormosh, I. Hunka, Y. Bazel, *Mat. Sci. Eng. C* 29 (2009) 1018.
38. M. Hasanzadeh, N. Shadjou, L. Saghatforoush, J. E. N. Dolatabadi, *Colloid. Surface B* 92 (2012) 91.
39. C. Liang, Y. Qin, C. Zhang, H. Lian, Y. Liu, *Guangzhou Chemical Industry* 45 (2017) 142.
40. X. Lin, G. Wang, S. Wang, C. Li, C. Yang, *Chin. J Pharm. Anal.* 29 (2009) 337